

## AUTOMATION OF THE LOCK ACQUISITION OF THE 3 KM ARM VIRGO INTERFEROMETER

*F.Acernese<sup>6</sup>, P.Amico<sup>10</sup>, M. Alshourbagy<sup>11</sup>, S.Aoudia<sup>7</sup>, S. Avino<sup>6</sup>, D.Babusci<sup>4</sup>, G.Ballardin<sup>2</sup>, F.Barone<sup>6</sup>, L.Barsotti<sup>11</sup>, M.Barsuglia<sup>8</sup>, F.Beauville<sup>1</sup>, M.A.Bizouard<sup>8</sup>, C.Boccaro<sup>9</sup>, F.Bondu<sup>7</sup>, L.Bosi<sup>10</sup>, C.Bradaschia<sup>11</sup>, S. Birindelli<sup>11</sup>, S.Braccini<sup>11</sup>, A.Brillet<sup>7</sup>, V.Brisson<sup>8</sup>, L.Brocco<sup>12</sup>, D.Buskulic<sup>1</sup>, E.Calloni<sup>6</sup>, E.Campagna<sup>3</sup>, F.Carbognani<sup>2</sup>, F.Cavalier<sup>8</sup>, R.Cavaliere<sup>2</sup>, G.Cella<sup>11</sup>, E.Chassande-Mottin<sup>7</sup>, C. Corda<sup>11</sup>, A.-C.Clapson<sup>8</sup>, F.Cleva<sup>7</sup>, J.-P.Coulon<sup>7</sup>, E.Cuoco<sup>2</sup>, V.Dattilo<sup>2</sup>, M.Davier<sup>8</sup>, R.De Rosa<sup>6</sup>, L.Di Fiore<sup>6</sup>, A.Di Virgilio<sup>11</sup>, B.Dujardin<sup>7</sup>, A.Eleuteri<sup>6</sup>, D.Enard<sup>2</sup>, I.Ferrante<sup>11</sup>, F.Fidecaro<sup>11</sup>, I.Fiori<sup>11</sup>, R.Flaminio<sup>1,2</sup>, J.-D.Fournier<sup>7</sup>, O.Francois<sup>2</sup>, S.Frasca<sup>12</sup>, F.Frasconi<sup>2;11</sup>, A. Freise<sup>2</sup>, L.Gammaitoni<sup>10</sup>, A.Gennai<sup>11</sup>, A.Giazotto<sup>11</sup>, G.Giordano<sup>4</sup>, L. Giordano<sup>6</sup>, R. Gouaty<sup>1</sup>, D. Grosjean<sup>1</sup>, G.Guidi<sup>3</sup>, S.Hebri<sup>2</sup>, H.Heitmann<sup>7</sup>, P.Hello<sup>8</sup>, L.Holloway<sup>2</sup>, S. Karkar<sup>1</sup>, S.Kreckelbergh<sup>8</sup>, P.La Penna<sup>2</sup>, N.Letendre<sup>1</sup>, V.Loriette<sup>9</sup>, M.Loupias<sup>2</sup>, G.Losurdo<sup>3</sup>, J.-M.Mackowski<sup>5</sup>, E.Majorana<sup>12</sup>, C.N.Man<sup>7</sup>, M. Mantovani<sup>11</sup>, F. Marchesoni<sup>10</sup>, F.Marion<sup>1</sup>, J. Marque<sup>2</sup>, F.Martelli<sup>3</sup>, A.Masserot<sup>1</sup>, M.Mazzoni<sup>3</sup>, L.Milano<sup>6</sup>, C. Moins<sup>2</sup>, J.Moreau<sup>9</sup>, N.Morgado<sup>5</sup>, B.Mours<sup>1</sup>, A. Pai<sup>12</sup>, C.Palomba<sup>12</sup>, F.Paoletti<sup>2;11</sup>, S. Pardi<sup>6</sup>, A. Pasqualetti<sup>2</sup>, R.Passaquieti<sup>11</sup>, D.Passuello<sup>11</sup>, B.Perniola<sup>3</sup>, F. Piergiovanni<sup>3</sup>, L.Pinard<sup>5</sup>, R.Poggiani<sup>11</sup>, M.Punturo<sup>10</sup>, P.Puppo<sup>12</sup>, K.Qipiani<sup>6</sup>, P.Rapagnani<sup>12</sup>, V.Reita<sup>9</sup>, A.Remillieux<sup>5</sup>, F.Ricci<sup>12</sup>, I.Ricciardi<sup>6</sup>, P. Ruggi<sup>2</sup>, G.Russo<sup>6</sup>, S.Solimeno<sup>6</sup>, A. Spallicci<sup>7</sup>, R.Stanga<sup>3</sup>, R. Taddei<sup>2</sup>, M. Tonelli<sup>11</sup>, A. Toncelli<sup>11</sup>, E.Tournefier<sup>1</sup>, F.Travasso<sup>10</sup>, G. Vajente<sup>11</sup>, D.Verkindt<sup>1</sup>, F.Vetrano<sup>3</sup>, A.Viceré<sup>3</sup>, J.-Y.Vinet<sup>7</sup>, H.Vocca<sup>10</sup>, M.Yvert<sup>1</sup>, Z. Zhang<sup>2</sup>*

<sup>1</sup>Laboratoire d'Annecy-le-Vieux de physique des particules, Chemin de Bellevue - BP 110, 74941 Annecy-le-Vieux Cedex - France

<sup>2</sup>European Gravitational Observatory (EGO), Via E. Amaldi, I-56021 Cascina (PI) Italia

<sup>3</sup>INFN - Sezione di Firenze/Urbino, Via G.Sansone 1, I-50019 Sesto Fiorentino and/or Università di Firenze, Largo E.Fermi 2, I - 50125 Firenze, and/or Università di Urbino, Via S.Chiera, 27, I-61029 Urbino, Italia

<sup>4</sup> INFN, Laboratori Nazionali di Frascati, Via E. Fermi, 40, I-00044 Frascati (Roma) - Italia

<sup>5</sup>LMA, 22, Boulevard Niels Bohr, 69622 - Villeurbanne- Lyon Cedex, France

<sup>6</sup>INFN - sezione di Napoli and/or Università di Napoli "Federico II", Complesso Universitario di Monte S. Angelo, Via Cinthia, I-80126 Napoli, Italia and/or Università di Salerno Via Ponte Don Melillo, I-84084 Fisciano (Salerno), Italia.

<sup>7</sup>Departement Artemis - Observatoire Cote d'Azur, BP 42209, 06304 Nice , Cedex 4, France

<sup>8</sup>Laboratoire de l'Accélérateur Linéaire (LAL),IN2P3/CNRS-Université de Paris-Sud, B.P. 34, 91898 Orsay Cedex - France

<sup>9</sup>ESPCI - 10, rue Vauquelin, 75005 Paris - France

<sup>10</sup>INFN Sezione di Perugia and/or Università di Perugia, Via A. Pascoli, I-06123 Perugia - Italia

<sup>11</sup>INFN - Sezione di Pisa and/or Università di Pisa, Via Filippo Buonarroti, 2 I-56127 PISA - Italia

<sup>12</sup> INFN, Sezione di Roma and/or Università "La Sapienza", P.le A. Moro 2, I-00185, Roma

Corresponding author e-mail address: franco.carbognani@ego-gw.it

### ABSTRACT

The aim of the VIRGO project is the detection of the gravitational waves emitted by astrophysical sources in a frequency range between few Hz and few kHz. The detector consist of a power recycled Michelson interferometer (ITF) with 3 km long Fabry-Perot cavities in its arms. To reduce the seismic disturbances, each optical component is suspended to a multi-pendulum system. In order to bring the detector in its working point (the detector "locking"), a complex procedure is required.

The mirrors should be aligned with an accuracy better than  $10^{-9}$  rad rms, and the relative distance of the suspended optics should be controlled with an accuracy better than  $10^{-12}$  m rms.

This working point of the detector is maintained using many feedback loops, working up to 10 kHz rate. The procedure to align and lock the detector, relying on hundreds of commands sent to several real-time processors, is done by a dedicated automation process. After a recall of the software and hardware environment, the automation effort is presented, together with the results obtained.

## INTRODUCTION

A simplified VIRGO optical layout is sketched in Fig.1. High-quality optics are suspended to act as quasi-free test masses at the end of the arms so that a gravitational wave, passing through the detector, would be visible in the ITF output signal [1]. The VIRGO large optics (mirrors and beam splitters) are suspended from a sophisticated seismic isolation system, the so-called superattenuator (SA) [2]. The SA consists of a multistage pendulum and offers an enormous passive isolation from seismic motion. However, the motion at the resonance frequencies (between 10 mHz and 4 Hz) can be large and must be reduced by active controls. The ITF has to be brought in the working position that is to have the laser light resonating in the Fabry-Perot and recycling cavity and the main output port on the dark fringe. This is achieved by steering all optical components in position and orientation via several real-time local and global controls with a bandwidth up to 10 kHz. VIRGO is a complex machine and bringing it into his final working conditions require elaborated procedures thus large automation support built on two automation layers:

- A real-time and fast automation layer directly implemented into the sub-system servers involved in the different loops.
- A control and monitoring automation layer qualifying the different subsystems using the control and monitoring channels collected by the *DAQ* and a script-like language to drive the different phases of the automation procedure, including lock acquisition.

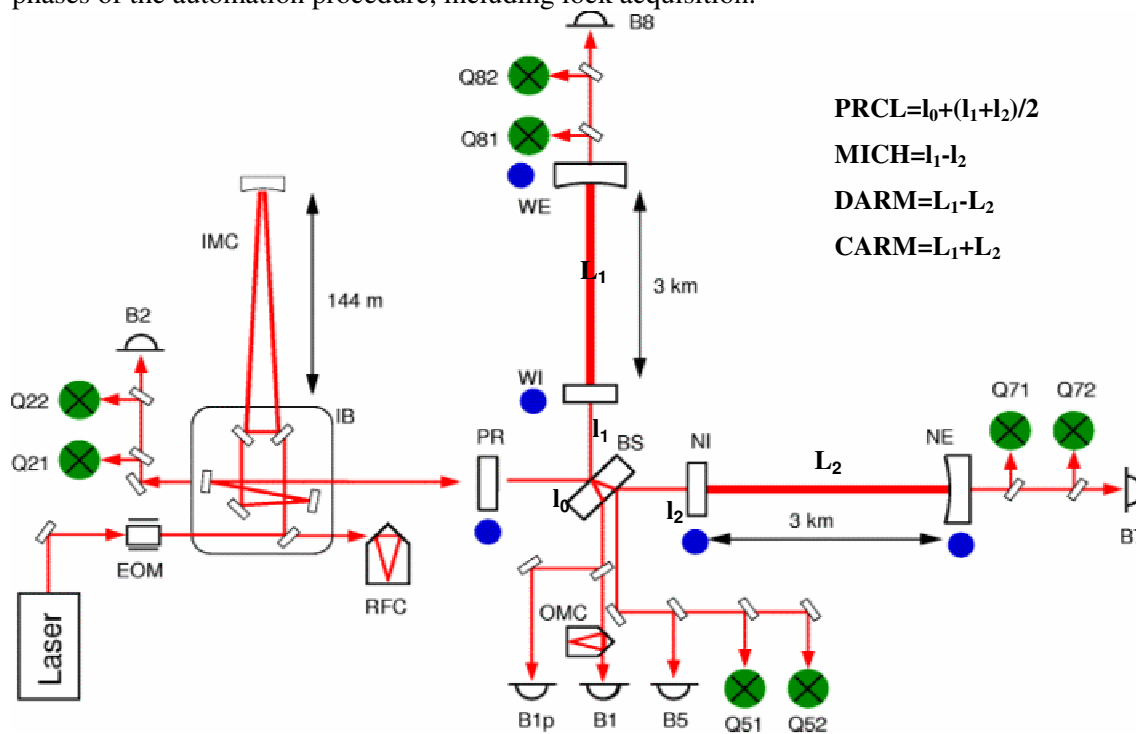


Fig.1 VIRGO Optical Layout, the mirrors (NI, NE, BS, ...) as well as the optical benches equipped with photodiodes (Bi) and quadrant photodiodes (Qi) are shown

## DATA ACQUISITION SYSTEM (DAQ)

The *DAQ*[5] collects the main ITF output (dark fringe signal) at 20 KHz, the data generated by the various ITF control systems and the data from the environmental noise. The control flags, the input error signals, the control algorithm results and the excitation signals are permanently collected to monitor the control loops. The collected data have a frequency range from few mHz up to 20KHz. The continuous data flow is around 18MBytes/s, reduced to 6MBytes/s thanks to the loss-less data compression. The data related to the same period of time are formatted into *frame*[6], 1 second long. The *Timing* system [7] samples synchronously the data over all the ITF and provides the time stamp for the frames. The frames, encapsulated by the VIRGO inter-processes communication Cm protocol [8], are sent to the frame builder stage using TCP/IP on an Ethernet network. The data are then

available for online visualizations (*dataDisplay*) or online computations with a short latency (mean value  $\approx 2$ -3s). Thank to the DAQ design, the frequent modifications in the control systems, new channels or sampling frequency modification, are easily handled.

## REAL-TIME AND FAST AUTOMATION LAYER

The digital control loops belonging to this layer are spread over the different VIRGO Subsystems and run either on dedicated Motorola PowerPC-based CPUs boards (RIO) or on custom DSP board (Motorola DSP96002-based). In the DSP case a server running on a RIO (EServerDSP) would provide the control/command interface. The control scheme or parameters can be modified by sending commands via the Cm protocol to the involved servers. Control loops data are sent through a digital optical link (DOL) to the DAQ system. The interaction between the two automations layers is thus implemented via Cm commands and DAQ channels

## CONTROL AND MONITORING AUTOMATION LAYER

### Automation of locking procedure (ALP)

The basic concept is to use the data acquired by the DAQ and to compute on a standard workstation the state of any subsystem by processing the collected channels related to it. According to the subsystem state, actions can be performed using the *system* calls or directly with messages in Cm format [8],.

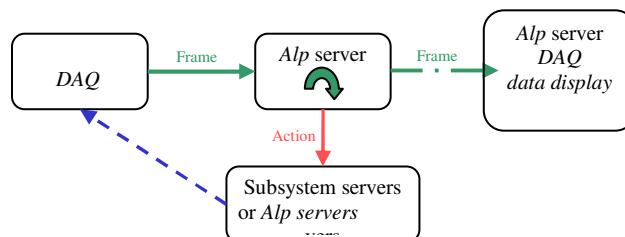


Fig.2 ALP architecture

The ALP server uses the DAQ framework to access the data and to report on the performed actions. It uses the *macro* concept to define a set of code related to the same automation phase and a script language to define the macro's content. Inside one macro, several functionalities can be used:

- ALP variables declaration,
- new DAQ channels can be created by performing arithmetic operation (+,-,\*,/) between input channels,
- DAQ channel's properties can be computed in the time domain (*mean,min,max,rms,range*) or in frequency domain (*FFT, bandRMS ...*) and stored into ALP variables,
- Arithmetic operations (+,-,\*,/) between ALP variables,
- test and loop conditions on ALP variables,
- commands can be sent to act on given sub-system servers,
- direct call of a *macro*

Using a set of macros, one can easily define any automation procedure. In order to better distribute the computational load and to provide a clean hierarchical organization (subsystems linked) to the different automation tasks, an architecture based on several ALP servers has been defined. When ALP was introduced it was considered useful for debugging and development reasons to have the whole automated procedure spitted into several macros called from a master Alp server that controls slave Alp servers.

## GLOBAL CONTROL

The Global Control [3] is a fully digital system in charge of the Locking and Alignment of the ITF. The Locking loop runs at 10 kHz while the Alignment one is synchronized at 500 Hz. Gc receives the digital information acquired by the photodiodes (for Locking) and by the quadrant photodiodes (for Alignment), computes the lengths or the angles to control (Sensing part), applies the correction filters

(Filtering part) and sends these corrections to the suspensions DSP that controls the mirrors (Driving part, only for Locking). Gc also computes the trigger conditions to enable the SSFS.

Gc is the place where the main control strategies are implemented. Moreover, in case of problem, it propagates the information to the suspensions controls that opens the loops avoiding the excitation of the system.

It has been designed to be able to switch between algorithms (Sensing, Filtering or Driving) in a smooth way without losing the control. On the other hand, some critical parameters of the algorithms can be changed “on-the-fly” without any disturbance. Those features are extensively used within ALP during the automated lock acquisition sequence and triggered via Cm commands sent to the Gc supervisor. Gc state transitions are also driven by ALP as soon as needed preconditions are fulfilled.

## INJECTION SYSTEM

Many control loops need to be fully coordinated for this system. The laser beam is filtered by a suspended triangular cavity, the *Input Mode Cleaner* (IMC), before being injected into the main ITF. The IMC is used as a reference in the pre-stabilization loop, while frequency stability below 15 Hz is achieved by an additional control system that stabilizes the length of the IMC with respect to a rigid 30 cm-long *reference cavity* (RFC), located on the suspended Input Bench (IB). A digital control loop, the Automatic Beam Positioner (ABP), allows the auto-alignment of the laser beam on the RFC. Once the ITF is locked, the laser frequency stabilization loop (SSFS) is engaged (and disengaged when needed) by the Global Control on one of the ITF error signal. In case of problems ALP can also disengage the loop within few seconds delay. More in general at ALP level many monitoring and recovery actions are implemented. The ABP loop is engaged and the RFC locked by ALP during the initialization phase (macro “General\_Init”) .

## MIRROR LOCAL CONTROLS

A digital control system using LVDTs and accelerometers as a monitor and acting at level of the SA top stage through coil-magnet actuators is implemented to damp the SA normal modes (*inertial damping*) [4]. Another digital control system using a ground-based camera and PSD as a monitor acts at mirror level through coil-magnet actuators (*local controls*). The two controls allow to reduce the pitch and yaw motions of each suspended mirror from several  $\mu\text{rads}$  down to fractions of  $\mu\text{rad}$ . This angular stability allows the pre-alignment of the beams in the ITF and the achievement of a stable interference pattern. In addition, those controls allow to reduce the longitudinal mirror speed along the beam direction down to  $1\mu\text{m}/\text{sec}$ . This longitudinal damping is needed to make smaller the dynamics of compensation force to be applied on the mirror.

Another large effect to be corrected at suspension level is the earth tide; this natural phenomenon changes the 3 km arm length by up to 200  $\mu\text{m}$ , with a 12 hours period. These large drifts of the mirrors are compensated by the Tidal Control loop that acts on the SA top stage. Among other actions, during the locking acquisition ALP take care of switching off the inertial damping loops, swapping from local controls to angular drift controls and switching the coil drivers to low noise mode.

## THE LOCK ACQUISITION PROCEDURE

The goal of the lock acquisition procedure is to bring the ITF on its working point, by controlling its 4 independent longitudinal lengths showed in Fig. 1:

- the length of the recycling cavity (PRCL),  $l_0 + (l_1 + l_2)/2$
- the differential length of the short Michelson arms (MICH),  $l_1 - l_2$ ;
- the common mode length (CARM)  $L1 + L2$  and the differential mode length (DARM)  $L1 - L2$  of the two long arms.

By using a carrier beam phase modulated at 6 MHz and the Pound-Drever-Hall technique [9] all the four lengths can be reconstructed by mixing the signals coming from photodiodes placed at different output ports of the interferometer.

For the ITF locking a novel strategy, called Variable Finesse Locking [10], has been adopted, in which the full control is sequentially reached through several steps.

The lock acquisition procedure embeds this strategy and consists of two main sequences, detailed below.

### Pre-alignment sequence

This sequence, not always executed at each lock acquisition attempt, is implemented by the following three macros:

- “Direct\_Beam\_Alignment”: Alignment of the direct beam into the North and the West arms.
- “Cavities\_Alignment”: North and West arm cavities independent locking, their non-linear alignment (when really needed) and their linear alignment.
- “PR\_Coarse\_Alignment”: Non-linear alignment of the Power Recycling (PR) mirror, with respect to the arm cavities mirrors aligned in the previous macro.

### Locking sequence

This sequence is implemented by a single macro, called “Lock\_Step\_request”. This macro takes as input parameter the step number to be reached. Here is detailed this multi-step sequence. Many of the listed actions corresponds mainly to Cm commands sent to ITF subsystems

- STEP 1 : Lock acquired with the PR mirror misaligned by 10  $\mu$ rads and the ITF on the grey fringe (i.e. Dark Fringe at 50%)
- STEP 2 : A boost filter added to the PRCL and MICH loops. Dark Fringe from 50 to 40%.
- STEP 3 : CARM loop controlled by the SSFS.
- STEP 4 : PR mirror aligned and consequently the power stored in the ITF increases
- STEP 5 : Dark Fringe from 40 to 20%. A boost filter is added to DARM loop.
- STEP 6 : Dark Fringe from 20 to 8%.
- STEP 7 : Dark Fringe from 8 to 5%.
- STEP 8 : Final step to Dark Fringe. Transition of the MICH loop error signal from the B1p DC signal to the B5 demodulated. Angular drift control switched on.
- STEP 9 : Transition of DARM loop error signal from the noisy B8 to the less noisy B1p demodulated.
- STEP 10 : Output Mode Cleaner (OMC) put on resonance, transition of DARM loop error signal from B1p to B1. After the transition all the noisy mirror motion dampers are switched off.
- STEP 11 : A filter having a reduced band and a high roll-off is added the MICH loop.
- STEP 12 : Activation of the tidal control, swapping to low-noise coil drivers.
- STEP 13 : Re-adjustment of demodulation phase and gain of PRCL loop.
- STEP 14 : A fraction of the MICH correction signal is sent in counter-phase to the end mirrors.
- STEP 15 : Permanent lines are added to the different mirror corrections for ITF calibration.

During the sequence execution and after its completion, a special macro, named “LockGuard”, working in background, watches for any unlock event. In case of unlock, it brings the ITF to the lock acquisition pre-conditions, avoiding also sub-systems over-excitations.

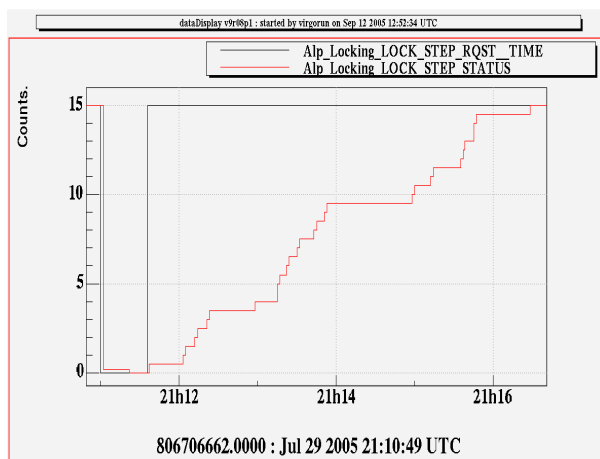


Fig.3 Locking status value transitions during the full locking sequence. Values correspond to the locking step numbers detailed before

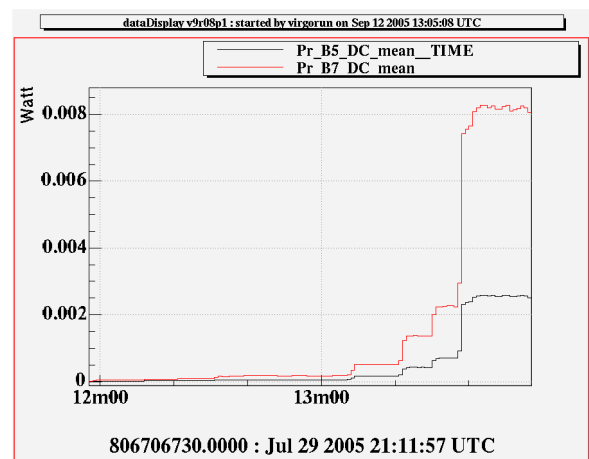


Fig.4 Power into the North arm cavity (B7) and the recycling cavity (B5) during the locking sequence.

## AUTOMATION PERFORMANCES

The performances obtained by the automation on the last engineering run C6, are very satisfactory. Fig.3 details the locking status value transitions during a typical alignment/locking sequence,. It can be noticed that the whole procedure is completed in less than 5 minutes. The evolution of the power inside the cavities is shown in Fig.4. During C6, the ITF has shown good stability with long stretch of continuous locking. But automation, and the very short recovery time after a delock has been one of the key elements to achieve the very high duty-cycle detailed in Fig. 5.

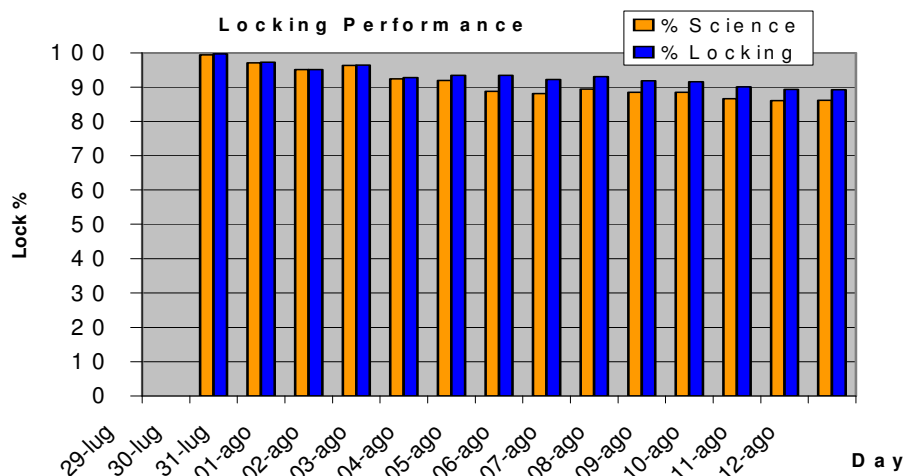


Fig.5 Duty cycle during the C6 run.

## CONCLUSIONS

As mentioned on the Performance chapter, in particular during the last engineering run, the automation has showed all his effectiveness in supporting the ITF operation. The Virgo machine is now provided with a tool allowing the operator to easily, reliably and quickly drive the machine into the working state. The next planned improvements are:

- Adding more controls and checks inside macros and modify some servers to allow them to provide their status and to confirm the correct handling of the requested commands. This should lead to a better recovering of an automated subsystem failure and a more efficient automated re-locking.
- Performing optimisation on critical servers currently generating latency peaks.

## REFERENCE

- [1] F. Acernese et al., "Status of Virgo", Proc. of the 6<sup>th</sup> Amaldi Conf. (2005).
- [2] G.Ballardin et al., "Measurement of the VIRGO Superattenuator performance for seismic noise suppression" Rev. Sci. Instrum., 79 (9), 3643-3652 (2001).
- [3] N.Arnaud et al, "The global control of the Virgo experiment", NIMA Vol550, p 467 (2005).
- [4] G.Losurdo et al., "Inertial control of the mirror suspensions of the VIRGO interferometer for gravitational wave detection" Rev. Sci. Instrum., 79 (9), 3653-3661 (2001).
- [5] F. Acernese et al., "The Virgo Data Acquisition System Software", Electronics 13th IEEE-NPSS Real Time Conference Montreal 22/07/03.
- [6] LIGO data group and Virgo data acquisition group, "Specification of a Common Data Frame Format for Interferometric Gravitational Waves Detectors", LIGO-T970130-F-E, VIR-SPE-APP-5400-102, <http://www.lapp.in2p3.fr/virgo/FrameL/>.
- [7] F.Bellachia, D.Boget, B.Mours, D.Verkindt, "The VIRGO Timing system ", VIR-LAP-5200-103 (1997).
- [8] C.Arnault, P. Massartal "A multitask communication package", - Orsay, France.
- [9] R.W.P.Drever et al., Appl. Phys. B : Photophys. Laser Chem., 31, 97-105 (1983).
- [10] F. Acernese et al., "The variable finesse locking technique "Proc. of the 6<sup>th</sup> Amaldi conference (2005)